Dyes and Pigments 116 (2015) 1–12

Contents lists available at ScienceDirect

Dyes and Pigments

journal homepage: www.elsevier.com/locate/dyepig

Incorporation of novel azobenzene dyes bearing oligo(ethylene glycol) spacers into first generation dendrimers

Jesús Ortíz-Palacios, Efraín Rodríguez-Alba, Gerardo Zaragoza-Galán, Jorge Rafael León-Carmona, Ana Martínez, Ernesto Rivera*

Instituto de Investigaciones en Materiales, Universidad Nacional Autónoma de México, Ciudad Universitaria, C.P. 04510 D.F. México, Mexico

ARTICLE INFO

Article history:
Received 16 May 2014
Received in revised form
10 September 2014
Accepted 25 November 2014
Available online 13 January 2015

Keywords:
Azobenzene
Dedrimers
Synthesis
Optical properties
Photoisomerization
Photoprotonation

ABSTRACT

Herein, we report the synthesis and inclusion of a new series of azo-dyes into first generation Fréchet type dendrimers. The incorporated dyes are amino-nitro, amino-methoxy and amino-butyl substituted azobenzenes bearing a well defined oligo(ethylene glycol) side chain. The optical properties of the dendrimers were studied by absorption spectroscopy. Dendrimer bearing amino-nitro substituted azobenzenes (λ = 480 nm in $CHCl_3$) behaved as a pseudostilbene type azobenzene whereas the others (λ = 409 nm in $CHCl_3$) showed the typical behaviour of aminoazobenzenes. Moreover, the *trans–cis* photoisomerization of the dendrimers was studied by UV–vis spectroscopy by irradiating at two different wavelengths (254 and 365 nm). In chloroform, the appearance of an intense red-shifted band revealed the presence of a photoprotonation effect in the azobenzene moiety. This phenomenon was also studied by absorption spectroscopy in function of time. The results were compared to those predicted by molecular modelling using Density Functional Theory calculations.

1. Introduction

Nowadays, dendrimers and dendrons have been considered one of the most attractive research fields in polymer chemistry due to their well-defined structures, versatility and potential applications [1–4]. These molecules can be modified by introducing functional groups and specific units at different levels of their structure: core, branches or periphery [5], giving rise to well-structured and highly functionalized molecules. Depending on the type of functional groups present in dendrimers, different properties have been already investigated, such as response to light. Some reviews include the first reports of photo-responsive dendrimers [6–9] giving many examples of azo-dendrimers. The most recent review covering the most important aspects of azobenzene containing dendrons and dendrimers, has been published by Caminade and Deloncle [10].

Azobenzenes had been used as terminal groups of dendrimers and dendrons, being the first examples those described by Vögtle and co-workers [11]. The first structures were prepared from poly(propyleneimine) (PPI) dendrimers built from either ethylenediamine [12] or 1,4-diaminobutane [1–14] as core. In most of the cases, all the terminal groups were azobenzenes [15–18].

The most popular types of dendrimers, poly(amidoamine) [19] and poly(arylether) [20], have been rarely used as support of azobenzene moieties. The first example of Fréchet type azodendrimers was synthesized by grafting through their core poly(-arylether) dendrons bearing a single azobenzene group on the surface, leading to original dendrimers [21–23] with azobenzene as terminal groups. Moreover, dendrons have not been frequently functionalized with azobenzenes on their periphery. The first example was used as building block for dendrimers [21,22]. More sophisticated systems, such as polyether dendrons linked to fullerenes, had been also prepared [24].

Rau classified azobenzenes into three main categories based on their photochemical behaviour [25]. Unsubstituted photochromic azobenzene makes up the first category, known as “azobenzenes”. The thermally stable *trans* isomer exhibits a strong $\pi-\pi^*$ transition at 350 nm and a weak $n-\pi^*$ transition at 440 nm, whereas the *cis* isomer undergoes similar transitions but with a more intense $n-\pi^*$ band. Moreover, “azobenzenes” have a relatively poor $\pi-\pi^*$ and $n-\pi^*$ overlap. The second category, known as “aminoazobenzenes” typically includes azobenzenes that are substituted by an electron-donor group and are characterized by the overlapping of the $\pi-\pi^*$ and $n-\pi^*$ bands. Finally, azobenzenes bearing both electron-donor

* Corresponding author. Tel.: +52 55 5622 4733; fax: +52 55 5616 1201.
E-mail address: riverage@unam.mx (E. Rivera).

http://dx.doi.org/10.1016/j.dyepig.2014.11.023
0143-7208/

and electron-acceptor groups belong to the third category, "pseudostilbenes", where the $\pi-\pi^*$ and $n-\pi^*$ bands are practically superimposed and inverted on the energy scale with respect to the "azobenzenes" bands [25].

When donor–acceptor substituted azobenzenes are incorporated into a polymer backbone or side-chain, they constitute versatile materials for several applications. In particular, irradiation with linear polarized light produces rapid *trans–cis–trans* photoisomerization of "pseudostilbene" azobenzenes. As a consequence, polarized light allows the selective activation of "pseudostilbenes" with polarization axis parallel to the absorbing radiation [26–32].

Azobenzene molecules can also undergo chromic changes through aggregation in various media including solution, spin-coated films and Langmuir–Blodgett multilayers. In these media, both H-type and J-type aggregates have been observed [33]. On the other hand, azobenzene and poly(ethylene glycol) have been employed in the synthesis of amphiphilic azo-dyes, copolymers [34,35], nanomaterials [36,37], cellulose derivatives [38,39] and cyclodextrin polymers [40,41], sometimes forming supramolecular complexes with interesting properties [42]. In fact, poly(ethylene glycol) segments provide flexibility and water solubility to the systems to which they are incorporated [43,44].

In the last ten years, our research group has worked on the synthesis and characterization of amphiphilic azo-dyes and azo-polymers bearing oligo(ethylene glycol) segments with different architectures. We reported the synthesis and characterization of four novel azo-dyes bearing terminal hydroxyl groups, the preparation of grafted azo-polymer films containing oligo(ethylene glycol) segments [45], and the synthesis and characterization of a new series of polymethacrylates bearing amino-nitro azobenzene units and oligo(ethylene glycol) chains their structure [46]. More recently, we published the synthesis and characterization of a series of liquid crystalline dyes bearing two amino-nitro substituted azobenzene units linked by well defined oligo(ethylene glycol) spacers [47].

Many articles about the preparation of new dendritic molecules containing azobenzene have been reported in the literature. Some of these materials exhibited outstanding optical properties, NLO response [48–54] or a liquid crystalline behaviour [55,56]. Last year, we reported the incorporation of amino-nitro substituted azobenzenes containing a tetra(ethylene glycol) side chain and other related dyes into dendritic structures, in order to get new liquid crystalline materials bearing azobenzene units. The thermal and optical properties of such dendrons were studied in detail, and some of them exhibited a liquid crystalline behaviour [57]. Herein, we report the incorporation of novel azo-dyes bearing amino-nitro, amino-methoxy and amino-butyl substituted azobenzenes into first generation Fréchet type dendrimers. The optical properties of these compounds, as well as the *trans–cis* photoisomerization and the photoprotonation effect, were studied by absorption spectroscopy. The results were compared to those predicted by molecular modelling using Density Functional Theory calculations. These new azo-dendrimers can be used for optical switching and storage as other azo-polymers previously reported in the literature. In addition, they can act as photochromic sensors since they exhibit noticeable colour changes arising from the photoinduced protonation which occur in $CHCl_3$ solution when they are irradiated with UV light at 254 nm.

2. Experimental

2.1. General conditions

All reagents used in the synthesis of the azo-dyes, dendrons and dendrimers were purchased from Aldrich and used as received without further purification. Acetone and dichloromethane were dried by distillation over calcium hydride. Precursor dyes (E)-2-(4-((4-nitrophenyl)diazenyl)phenyl)-5,8,11-trioxa-2-azatridecan-13-ol (**1**), (E)-2-(4-((4-methoxyphenyl)diazenyl)phenyl)-5,8,11-trioxa-2-azatridecan-13-ol (**2**) and (E)-2-(4-((4-butylphenyl)diazenyl)phenyl)-5,8,11-trioxa-2-azatridecan-13-ol (**3**) were synthesized according to the method previously reported by us [45], and the poly(aryl ether) dendrons were prepared as described in the literature [58]. FTIR spectra of the compounds were carried out on a Spectrum 100 (Perkin Elmer PRECISELY) spectrometer in solid state. ^1H and ^{13}C NMR spectra of these compounds in $CDCl_3$ solution were recorded at room temperature on a Bruker Avance 400 MHz spectrometer operating at 400 MHz and 100 MHz for ^1H and ^{13}C, respectively.

All dendrons were dissolved in spectral quality solvents purchased from Aldrich, and their absorption spectra were recorded on a Varian Cary 1 Bio UV–vis (model 8452A) spectrophotometer at room temperature, using 1 cm quartz cuvettes.

Photoisomerization and photoprotonation experiments of azo-dendrimers **14G$_1$** and **15G$_1$** were carried out in DMF and $CHCl_3$ solutions (2.5×10^{-5} M) at room temperature. The samples were irradiated with UV light using a Compact UV lamp model UVGL-25, 254/365 nm (6W). Each solution was irradiated at 254 and 365 nm for 5 min. The spectral changes were monitored by absorption spectroscopy with intervals of 5 s.

2.2. Computational and theoretical details

All calculations were carried out by using the Gaussian 09 implementation [59]. Calculations involving atomic geometry and electronic structure were performed by applying the Density Functional Theory (DFT) framework for all the stationary points, using the B3LYP [60] functional and the basis 6-31G [61–65]. In order to verify optimized minima, harmonic analyses were achieved and local minima were identified with zero imaginary frequencies. In order to simulate the UV–visible spectra, time-dependent DFT (TD-DFT) method was employed using the same methodology. The UV–visible spectra were obtained for half singlet and half triplet states, effective for closed-shell systems.

2.3. Synthesis

2.3.1. Synthesis of the precursor azo-dyes

Precursor azo-dyes (E)-2-(4-((4-nitrophenyl)diazenyl)phenyl)-5,8,11-trioxa-2-azatridecan-13-ol (**1**), (E)-2-(4-((4-methoxyphenyl)diazenyl)phenyl)-5,8,11-trioxa-2-azatridecan-13-ol (**2**) and (E)-2-(4-((4-butylphenyl)diazenyl)phenyl)-5,8,11-trioxa-2-azatridecan-13-ol (**3**) were prepared according to the method previously reported by us [45].

2.4. Synthesis of the dendrons

2.4.1. Synthesis of the 3-dodecyloxy-5-hydroxybenzyl alcohol (*8*)

The synthesis and characterization of the dendron (**8**) has been previously reported by us [57]. Yield: 68%.

FTIR (Film) υ/cm^{-1}: 3375 (OH), 2913, 2847 (CH_3, CH_2), 1595, 1469 (C=C, Ar), 1378, 1328 (CH_3, CH_2), 1305 (ArOCH), 1160 (COC) and 1037 (ArOCH).

^1H NMR (400 MHz, $CDCl_3$): $\delta = 6.35$ (s, $J = 2$ Hz, 2H, H^1-H^3), 6.28 (s, $J = 2$ Hz, 1H, H^2), 4.46 (s, 2H, $PhCH_2OH$), 3.80 (t, $J = 6.62$ Hz, 2H, $PhOCH_2$), 1.69 (m, 2H, $PhOCH_2CH_2$), 1.26 (m, 18H, all CH_2 of the aliphatic chain), 0.88 (t, $J = 6.56$ Hz, 3H, CH_3) ppm.

^{13}C NMR (100 MHz, $CDCl_3$): $\delta = 160.41$ (1C, C^b), 157.13 (1C, C^d), 142.67 (1C, C^f), 106.32 (1C, C^e), 105.49 (1C, C^a), 101.28 (1C, C^c), 68.13 (1C, $PhOCH_2C^e$), 64.91 (1C, $PhCH_2OH$), 31.88 (1C, $PhOCH_2CH_2$),

29.61, 29.41, 29.32, 29.18, 25.98, 22.64 (9C, all CH_2 of the aliphatic chain), 14.05 (1C, CH_3) ppm.

2.4.2. Synthesis of the iodided intermediates

Intermediates (**4**), (**5**) and (**6**) were obtained using the methodology reported by us [57] which is described only for (**4**).

(2-{2-[2-(2-Iodo-ethoxy)-ethoxy]-ethoxy}-ethyl)-methyl-[4-(4-nitro-phenylazo)-phenyl]-amine (**4**)

Compound (**1**) (4.37 g, 10.11 mmol)was reacted with imidazole (0.89 g, 13.1 mmol), triphenylphosphine (3.44 g, 13.1 mmol) and iodine (3.34 g, 13.1 mmol) in 50 mL anhydrous dichloromethane at room temperature. The resulting solution was stirred for 6 h, filtered and concentrated at reduced pressure. The crude product was purified by column chromatography in silica gel, using mixtures of ethyl acetate/hexane (4:6, 5:5, and 6:4) as eluent. Since this intermediate is very instable it was immediately used in the next reaction without further purification. Relative yield: 80%.

For (2-{2-[2-(2-Iodo-ethoxy)-ethoxy]-ethoxy}-ethyl)-[4-(4-methoxy-phenylazo)-phenyl]-methyl-amine (**5**): Relative yield: 85%.

For [4-(4-Butyl-phenylazo)-phenyl]-(2-{2-[2-(2-iodo-ethoxy)-ethoxy]-ethoxy}-ethyl)-methyl-amine (**6**): Relative yield: 85%.

2.4.3. Synthesis of [3-dodecyloxy-5-(2-{2-[2-(2-{methyl-[4-(4-nitro-phenylazo)-phenyl]-amino}-ethoxy)-ethoxy]-ethoxy}-ethoxy)-phenyl]-methanol (***9G$_1$OH***)

The dendrons **9G$_1$OH**, **10G$_1$OH** and **11G$_1$OH** were obtained employing the procedure previously reported by us [57]. For **9G$_1$OH**: Yield: 62%.

FTIR (Film) υ/cm^{-1}: 3452 (OH), 2921, 2852 (CH_3, CH_2), 1602, 1514 (C═C, Ar), 1455 (N═N), 1380 (CH), 1340 (NO_2), 1137 (ArOCH), 1102 (COC) and 1070 (ArOCH). MALDITOF: $C_{40}H_{58}N_4O_8$ Calcd: $[M+H]^+$ 722.91 Found (*m*/*z*): $[M+H]^+$ 722.47.

^{1}H NMR (400 MHz, CDCl3) (Scheme 1a): δ = 8.24 (d, *J* = 9.02 Hz, 2H, H^7), 7.84 (d, *J* = 9.05 Hz, 2H, H^6), 7.81 (d, *J* = 9.21 Hz, 2H, H^5), 6.70 (d, *J* = 9.23 Hz, 2H, H^4), 6.49 (d, *J* = 2 Hz, 2H, H^1–H^3), 6.37 (t, *J* = 2 Hz, 1H, H^2), 4.53 (s, 2H, $PhCH_2OH$), 4.03 (t, *J* = 4.99 Hz, 2H, $PhOCH_2$ of the tetra(ethylene glycol) chain), 3.84 (t, *J* = 6.58 Hz, 2H, $PhOCH_2$ of the aliphatic chain), 3.75 (t, *J* = 4.62 Hz, 2H, CH_2N), 3.64–3.57 (m, 12H, OCH_2 of the tetra(ethylene glycol) chain), 3.06 (s, 3H, CH_3N), 1.77–1.70 (m, 2H, $PhOCH_2CH_2$), 1.40–1.38 (m, 2H, $PhO(CH_2)_2CH_2$), 1.34–1.25 (m, 18H, all CH_2 of the aliphatic chain), 0.81 (t, *J* = 6.67 Hz, 3H, CH_3) ppm.

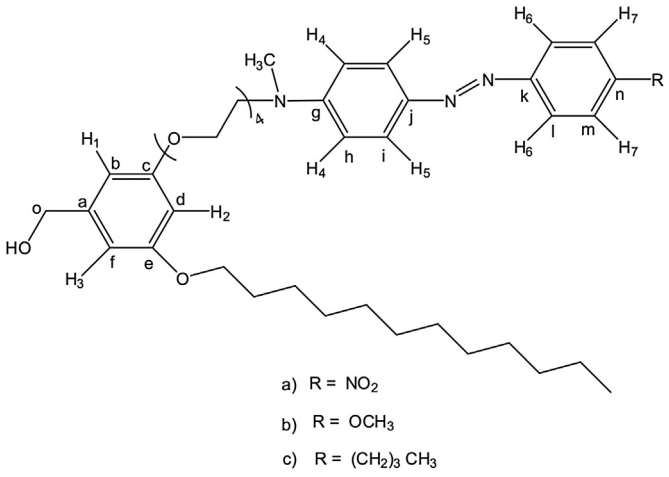

Scheme 1. Assignment of the signals for dendrons 9G1OH, 10G1OH and 11G1OH.

^{13}C NMR (100 MHz, CDCl3) (Scheme 1a): δ = 160.63 (1C, C^e), 160.22 (1C, C^c), 156.89 (1C, C^k), 152.67 (1C, C^g), 147.53 (1C, C^n), 143.92 (1C, C^j), 143.37 (1C, C^a), 126.08 (2C, C^i), 124.62 (2C, C^m), 122.59 (2C, C^l), 111.60 (2C, C^h), 105.60 (1C, C^f), 105.26 (1C, C^b), 101.04 (1C, C^d), 70.88–70.77, 69.80, 67.63 (6C, OCH_2), 68.68 (1C, $PhOCH_2$ aliphatic chain), 68.22 (1C, $PhOCH_2$ of the tetra(ethylene glycol) chain), 65.35 (1C, C^o), 52.31 (1C, NCH_2), 39.26 (1C, NCH_3), 31.91, 29.65–29.31, 26.06, 22.65 (10C, all CH_2 of the aliphatic chain), 14.03 (1C, CH_3) ppm.

2.4.4. Synthesis of the [3-dodecyloxy-5-(2-{2-[2-(2-{[4-(4-methoxy-phenylazo)-phenyl]-methyl-amino}-ethoxy)-ethoxy]-ethoxy}-ethoxy)-phenyl]-methanol (***10G$_1$OH***)

Yield: 64%.

FTIR (Film) υ/cm^{-1}: 3426 (OH), 2920, 2851 (CH_3, CH_2), 1594, 1514 (C═C, Ar), 1447 (N═N), 1376(CH), 1244 (ArOCH) and 1147 (ArOCH). MALDITOF: $C_{41}H_{61}N_3O_7$ Calcd: $[M+H]^+$ 707.96 Found: (*m*/*z*):$[M+H]^+$ 707.41.

^{1}H NMR (400 MHz, $CDCl_3$) (Scheme 1b): δ = 7.83 (d, *J* = 9.1 Hz, 2H, H^6), 7.73 (d, *J* = 8.7 Hz, 2H, H^5), 7.26 (d, *J* = 8.2 Hz, 2H, H^7), 6.76 (d, *J* = 9.1 Hz, 2H, H^4), 6.48 (d, *J* = 2 Hz, 2H, H^1–H^3), 6.37 (d, *J* = 2 Hz, 1H, H^2), 4.60 (s, 2H, $PhCH_2OH$), 4.08 (t, *J* = 4.54 Hz, 2H, $PhOCH_2$ of the tetra(ethylene glycol) chain), 3.90 (t, *J* = 6.57 Hz, 2H, $PhOCH_2$ of the aliphatic chain), 3.87 (s, 3H, $PhOCH_3$), 3.82 (t, *J* = 4.81 Hz, 2H, CH_2N), 3.69–3.62 (m, 12H, OCH_2), 3.11 (s, 3H, CH_3N), 1.77–1.70 (m, 2H, $PhOCH_2CH_2$), 1.45–1.38 (m, 2H, $PhO(CH_2)_2CH_2$), 1.34–1.26 (m, 16H, all CH_2 of the aliphatic chain), 0.884 (t, *J* = 6.56 Hz, 3H, CH_3) ppm.

^{13}C NMR (100 MHz, $CDCl_3$) (Scheme 1b): δ = 160.72 (1C, C^n), 160.34 (1C, C^e), 159.96 (1C, C^c), 150.90 (1C, C^g), 147.34 (1C, C^k), 143.51 (1C, C^j), 143.35 (1C, C^a), 124.49 (2C, C^i), 123.71 (2C, C^l), 113.99 (2C, C^m), 111.36 (2C, C^h), 105.30 (1C, C^f), 104.86 (1C, C^b), 100.56 (1C, C^d), 70.67–70.59, 69.62, 67.33 (6C, OCH_2), 68.46 (1C, $PhOCH_2$ of the aliphatic chain), 67.97 (1C, $PhOCH_2$ tetra(ethylene glycol) chain), 65.04 (1C, C^o), 55.39 (1C, NCH_2), 52.08 (1C, OCH_3), 39.10 (1C, NCH_3), 31.83, 29.58–29.16, 25.96, 22.60 (10C, all CH_2 of the aliphatic chain), 14.05 (1C, CH_3) ppm.

2.4.5. Synthesis of the [3-(2-{2-[2-(2-{[4-(4-butyl-phenylazo)-phenyl]-methyl-amino}-ethoxy)ethoxy]-ethoxy}-ethoxy)-5-dodecyloxy-phenyl]-methanol (***11G$_1$OH***)

Yield: 63%.

FTIR (Film) υ/cm^{-1}: 3420 (OH), 2921, 2852 (CH_3, CH_2), 1597, 1514 (C═C, Ar), 1447 (N═N), 1376(CH), 1155 (ArOCH), 1138 (COC), 1068 (ArOCH). MALDITOF: $C_{44}H_{67}N_3O_6$ Calcd: $[M+H]^+$ 733.50 Found: (*m*/*z*):$[M+H]^+$ 733.54.

^{1}H NMR (400 MHz, $CDCl_3$) (Scheme 1c): δ = 7.75 (d, *J* = 9.05 Hz, 2H, H^6), 7.67 (d, *J* = 8.29 Hz, 2H, H^5), 7.19 (d, *J* = 8.66 Hz, 2H, H^7), 6.67 (d, *J* = 9.14 Hz, 2H, H^4), 6.42 (t, *J* = 2 Hz, 2H, H^1–H^3), 6.31 (t, *J* = 2 Hz, 1H, H^2), 4.48 (s, 2H, $PhCH_2OH$), 4.08 (t, *J* = 4.39 Hz, 2H, $PhOCH_2$ of the tetra(ethylene glycol) chain), 3.91 (t, *J* = 6.55 Hz, 2H, $PhOCH_2$ of the aliphatic chain), 3.81 (t, *J* = 4.78 Hz, 2H, CH_2N), 3.69–3.60 (m, 12H, OCH_2), 3.08 (s, 3H, CH_3N), 2.65 (t, *J* = 7.7 Hz, 2H, $PhCH_2CH_2$), 1.78–1.71 (m, 2H, $PhOCH_2CH_2$), 1.66–1.59 (m, 2H, $PhCH_2$), 1.43–1.26 (m, 20H, $Ph(CH_2)_2CH_2$ and all CH_2 of the aliphatic chain), 0.93 (t, *J* = 7.33 Hz, 3H, CH_3), 0.87 (t, *J* = 6.71 Hz, 3H, $Ph(CH_2)_3CH_3$) ppm.

^{13}C NMR (100 MHz, $CDCl_3$) (Scheme 1c): δ = 160.45 (1C, C^e), 160.08 (1C, C^c), 151.37 (1C, C^g), 151.17 (1C, C^k), 144.66 (1C, C^n), 143.65 (1C, C^j), 143.29 (1C, C^a), 128.91 (2C, C^m), 124.79 (2C, C^i), 122.09 (2C, C^l), 111.39 (2C, C^h), 105.40 (2C, C^f), 104.98 (1C, C^b), 100.70 (1C, C^d), 70.78–70.69, 69.70, 68.54 (6C, OCH_2), 68.06 (1C, $PhOCH_2$ of the aliphatic chain), 67.44 (1C, $PhOCH_2$ of the tetra(ethylene glycol) chain), 65.27 (1C, C^o), 52.17 (1C, NCH_2), 39.21 (1C, NCH_3), 35.48 (1C, $PhCH_2$), 33.49 (1C, $PhCH_2CH_2$), 31.89, 29.60–29.31, 26.02, 22.64

(10C, all CH_2 of the aliphatic chain), 22.31 (1C, $Ph(CH_2)_2CH_2$), 14.07 (1C, CH_3), 13.89 (1C, $Ph(CH_2)_3CH_3$) ppm.

2.5. Synthesis of the dendrimers

The synthesis of the dendrimers **$13G_1$**, **$14G_1$** and **$15G_1$** is described only for **$13G_1$** and the spectroscopical characterization is given for all the compounds.

2.5.1. Tris(3-(dodecyloxy)-5-(2-(methyl(4-((E)-(4nitrophenyl) diazenyl)phenyl)amino) ethoxy) benzyl) benzene-1,3,5-tricarboxylate (***$13G_1$***)

The dendron (**$9G_1OH$**) (0.1476 g, 0.17 mmol) and triethylamine (0.023 mL, 0.51 mmol) were dissolved in 10 mL anhydrous CH_2Cl_2. A solution of 1,3,5-benzenetricarboxyl trichloride (0.016 g, 0.063 mmol) in 5 mL anhydrous CH_2Cl_2 was added dropwise. The reaction mixture was stirred out at room temperature for 4 days. Then, it was filtrated and evaporated at reduced pressure. The crude product was washed with water, extracted with chloroform and dried with anhydrous $MgSO_4$. The final product was evaporated at reduced pressure and purified by column chromatography in silica gel using mixtures ethyl acetate/hexane (5:5, 6:4 and 7:3) as eluent, to yield the first generation dendrimer **$13G_1$**. Yield: 31%.

FTIR (Film) υ/cm^{-1}: 2922, 2853 (CH_3, CH_2) 1727 (C═O), 1599, 1517 (C═C, Ar) and 1450 (N═N). MALDITOF: $C_{129}H_{174}N_{12}O_{27}$ Calcd: $[M+H]^+$ 2324.83. Found: (m/z): $[M+H]^+$ 2324.92.

^1H NMR (400 MHz, $CDCl_3$) (Scheme 2a): δ = 8.85 (s, 3H, H^8), 8.29 (d, J = 8.87 Hz, 6H, H^7), 7.88 (d, J = 8.96 Hz, 6H, H^6), 7.86 (d, J = 9.28 Hz, 6H, H^5), 6.74 (d, J = 9.04 Hz, 6H, H^4), 6.55 (d, J = 2 Hz, 6H, H^1–H^3), 6.42 (d, J = 2 Hz, 3H, H^2), 5.28 (s, 6H, $PhCOOCH_2Ph$), 4.08 (t, J = 3.55 Hz, 6H, $PhOCH_2$ of the tetra(ethylene glycol) chain), 3.90 (t, J = 6.37 Hz, 6H, $PhOCH_2$ of the aliphatic chain), 3.81 (t, J = 4.54 Hz, 6H, CH_2N), 3.68–3.61 (m, 36H, OCH_2), 3.10 (s, 9H, CH_3N), 1.76–1.69 (m, 6H, $PhOCH_2CH_2$), 1.44–1.39 (m, 6H, $Ph(CH_2)_2CH_2$), 1.32–1.24 (m, 54H, all CH_2 of the aliphatic chain), 0.87 (t, J = 6.24 Hz, 9H, CH_3) ppm.

^{13}C NMR (100 MHz, $CDCl_3$) (Scheme 2a): δ = 164.66 (3C, C^r), 160.57 (3C, C^e), 160.14 (3C, C^c), 156.81 (3C, C^k), 152.58 (3C, C^g), 147.42 (3C, C^n), 143.81 (3C, C^j), 137.58 (3C, C^a), 134.84 (3C, C^p), 131.26 (3C, C^q), 126.07 (6C, C^i), 124.62 (6C, C^m), 122.57 (6C, C^l), 111.52 (6C, C^h), 107.09 (3C, C^f), 106.70 (3C, C^b), 101.49 (3C, C^d), 70.85–70.71, 68.21 (18C, OCH_2), 69.68 (3C, $PhOCH_2$ of the aliphatic chain), 68.61 (3C, $PhOCH_2$ of the tetra(ethylene glycol) chain), 67.56 (3C, C^o), 52.23 (3C, NCH_2), 39.30 (3C, NCH_3), 31.90, 29.66–29.26, 26.05, 22.66 (30C, all CH_2 of the aliphatic chain), 14.08 (3C, CH_3) ppm.

2.5.2. Tris(3-(dodecyloxy)-5-(2-((4-((E)-(4 methoxyphenyl) diazenyl)phenyl) (methyl)amino) ethoxy)benzyl) benzene-1,3,5-tricarboxylate (***$14G_1$***)

Yield: 29%.

FTIR (Film) υ/cm^{-1}: 2921, 2852 (CH_3, CH_2), 1726 (C═O), 1595, 1513 (C═C, Ar) and 1448 (N═N). MALDITOF: $C_{132}H_{183}N_9O_{24}$ Calcd: $[M+H]^+$ 2279.91 Found: (m/z): $[M+H]^+$ 2280.17.

^1H NMR (400 MHz, $CDCl_3$) (Scheme 2b): δ = 8.87 (s, 3H, H^8), 7.81 (d, J = 9.05 Hz, 6H, H^6), 7.79 (d, J = 9.05 Hz, 6H, H^5), 6.96 (d, J = 9.05 Hz, 6H, H^7), 6.73 (d, J = 9.05 Hz, 6H, H^4), 6.56 (t, J = 2 Hz, 6H, H^1–H^3), 6.43 (t, J = 2 Hz, 3H, H^2), 5.29 (s, 6H, $PhCOOCH_2Ph$), 4.08 (t, J = 4.54 Hz, 6H, $PhOCH_2$ of the tetra(ethylene glycol) chain), 3.91 (t, J = 6.54 Hz, 6H, $PhOCH_2$ of the aliphatic chain), 3.85 (s, 9H, $PhOCH_3$), 3.81 (t, J = 4.94 Hz, 6H, CH_2N), 3.69–3.58 (m, 36H, OCH_2), 3.06 (s, 9H, CH_3N), 1.77–1.70 (m, 6H, $PhOCH_2CH_2$), 1.45–1.37 (m, 6H, $PhO(CH_2)_2CH_2$), 1.33–1.25 (m, 48H, all CH_2 of the aliphatic chain), 0.88 (t, J = 6.72 Hz, 9H, CH_3) ppm.

^{13}C NMR (100 MHz, $CDCl_3$) (Scheme 2b): δ = 164.72 (3C, C^r), 160.82 (3C, C^n), 160.50 (3C, C^e), 160.11 (3C, C^c), 150.99 (3C, C^g), 147.38 (3C, C^k), 143.60 (3C, C^j), 137.55 (3C, C^a), 134.91 (3C, C^p), 131.21

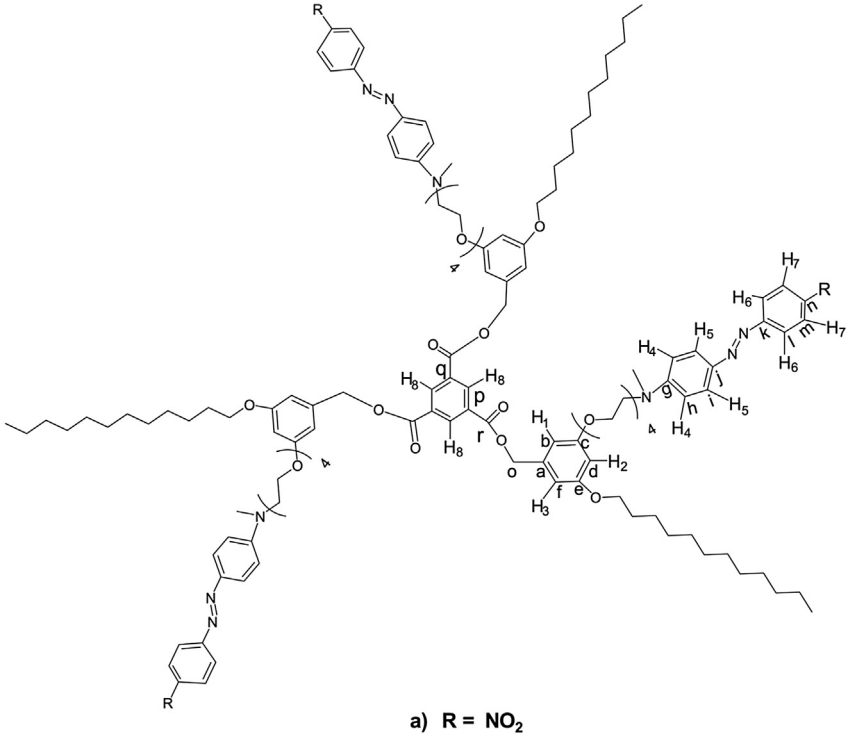

Scheme 2. Assignment of the signals for dendrimers 13G1, 14G1 and 15G1.

(3C, C^q), 124.65 (6C, C^i), 123.82 (6C, C^l), 114.09 (6C, C^m), 111.49 (6C, C^h), 107.08 (3C, C^f), 106.62 (3C, C^b), 101.36 (3C, C^d), 70.75–70.62, 69.60, 67.41 (18C, OCH_2), 68.49 (3C, $PhOCH_2$ of the aliphatic chain), 68.09 (3C, $PhOCH_2$ of the tetra(ethylene glycol) chain), 67.24 (3C, C^o), 55.45 (3C, NCH_2), 52.15 (3C, OCH_3), 39.20 (3C, NCH_3), 31.88, 29.64–29.20, 26.01, 22.65 (30C, all CH_2 of the aliphatic chain), 14.10 (3C, CH_3) ppm.

*2.5.3. Tris(3-(2-((4-((E)-(4-butylphenyl)diazenyl)phenyl)(methyl) amino)ethoxy)-5 (dodecylo-xy)benzyl)benzene-1,3,5-tricarboxylate (**15G$_1$**)*

Yield: 29%.

FTIR (Film) υ/cm^{-1}: 2923, 2853 (CH_3, CH_2), 1726 (C=O), 1596, 1514 (C=C, Ar) and 1446 (N=N). MALDITOF: $C_{132}H_{183}N_9O_{24}$ Calcd: $[M+H]^+$ 2358.15. Found: (*m*/*z*):$[M+H]^+$ 2359.14.

^{1}H NMR (400 MHz, $CDCl_3$) (Scheme 1c): δ = 8.87 (s, 3H, H^8), 7.82 (d, *J* = 8.98 Hz, 6H, H^6), 7.74 (d, *J* = 8.23 Hz, 6H, H^5), 7.26 (d, *J* = 8.23 Hz, 6H, H^7), 6.73 (d, *J* = 9.03 Hz, 6H, H^4), 6.56 (d, *J* = 2 Hz, 6H, H^1–H^3), 6.44 (t, *J* = 2 Hz, 3H, H^2), 5.29 (s, 6H, $PhCOOCH_2Ph$), 4.09 (t, *J* = 4.25, 6H, $PhOCH_2$ of the tetra(ethylene glycol) chain), 3.91 (t, *J* = 6.44 Hz, 6H, $PhOCH_2$ of the aliphatic chain), 3.82 (t, *J* = 4.46 Hz, 6H, CH_2N), 3.68–3.61 (m, 36H, OCH_2), 3.06 (s, 6H, CH_3N), 2.66 (t, *J* = 7.62 Hz, 2H, $PhCH_2CH_2$), 1.76–1.70 (m, 6H, $PhOCH_2CH_2$), 1.66–1.58 (m, 6H, $PhCH_2$), 1.41–1.25 (m, 60H, $Ph(CH_2)_2CH_2$ and all CH_2 of the aliphatic chain), 0.94 (t, *J* = 7.33 Hz, 6H, CH_3), 0.88 (t, *J* = 6.48 Hz, 3H, $Ph(CH_2)_3CH_3$) ppm.

^{13}C NMR (100 MHz, $CDCl_3$) (Scheme 1c): δ = 164.79 (3C, C^r), 160.61 (3C, C^e), 160.21 (3C, C^c), 151.51 (3C, C^g), 151.28 (3C, C^k), 144.75 (3C, C^n), 143.79 (3C, C^j), 137.66 (3C, C^a), 134.99 (3C, C^p), 131.33 (3C, C^q), 129.03 (6C, C^m), 124.91 (6C, C^l), 122.24 (6C, C^i), 111.50 (6C, C^h), 107.18 (6C, C^f), 106.72 (3C, C^b), 101.49 (3C, C^d), 70.53–70.35, 69.37, 67.21 (18C, OCH_2), 68.28 (3C, $PhOCH_2$ of the aliphatic chain), 67.87 (3C, $PhOCH_2$ of the tetra(ethylene glycol) chain), 67.01 (3C, C^o), 51.89 (3C, NCH_2), 38.93 (3C, NCH_3), 35.22 (3C, $PhCH_2$), 33.24 (3C, $PhCH_2CH_2$), 31.64, 29.40–29.08, 28.08, 25.78, 22.41 (30C, all CH_2 of the aliphatic chain), 22.06 (3C, $Ph(CH_2)_2CH_2$), 13.86 (3C, CH_3), 13.68 (3C, $Ph(CH_2)_3CH_3$) ppm.

3. Results and discussion

3.1. Synthesis of the dendrimers

The synthesis of the dendrimers was achieved using the convergent approach and is illustrated in Fig. 1. Three different series of first generation Fréchet type dendrimers bearing azobenzene units in the periphery were prepared employing 3,5-dihydroxy benzylic alcohol as built unit. The dendrimers were obtained by coupling 3.2 eq of the precursor dendrons (**G$_1$OH**) in the presence of 1 eq of the reactive 1,3,5-benzenetricarboxyl trichloride. The first series of dendrimers were funcionalized with (amino-nitro), (amino-methoxy) and (amino-butyl) substituted azobenzenes.

Precursor azobenzenes (**1**), (**2**) and (**3**) have been prepared according to the method previously reported by us [45]. These compounds were treated in the presence of iodine, imidazole and PPh_3 to give the corresponding alkyl iodides (**4**), (**5**) and (**6**). On the other hand, 3,5-dihydroxy benzylic alcohol (**7**) (1 eq) was reacted in the presence of 1-dodecyl bromide (1 eq) using K_2CO_3 as base and acetone as solvent, with a catalytic amount of 18-crown-6 to give the asymmetric dendron (**8**). This compound was further reacted with intermediate (**4**), using K_2CO_3 as base and DMF as solvent in the presence of 18-crown-6 to give the first generation dendron **9G$_1$OH**. Finally, **9G$_1$OH** was reacted with 1,3,5-benzenetricarboxyl trichloride (3.2 eq) in the presence of Et_3N to give first generation dendrimer(**13G$_1$**). Similarly, other two series of first generation dendrimers were prepared from (**5**) and (**6**) under the same reaction conditions described above to give the corresponding dendrons **14G$_1$** and **15G$_1$**, respectively (Fig. 1).

3.2. Characterization of the dendrimers

The precursor azo-dyes, dendrons and dendrimers were fully characterized by ^{1}H and ^{13}C NMR spectroscopies, and the molecular weights and purity of the final products were confirmed by MALDI-TOF mass spectrometry using dithranol as matrix. The ^{1}H NMR and ^{13}C NMR spectra of the dendrimer bearing amino-methoxy substituted azobenzene units (**14G$_1$**) are shown in Fig. 2, but the spectroscopic data of all compounds are given in the experimental section. The ^{1}H NMR and ^{13}C NMR of all dendrimers can be found in the Supporting Information (SI).

In the ^{1}H NMR spectrum of **10G$_1$OH** (SI, Fig. S2), there are six signals in the aromatic region at 7.87, 7.73, 7.26, 6.76, 6.50 and 6.37 ppm due to the aromatic protons present in the azobenzene unit and phenyl group H^6, H^7, H^4, H^1–H^3 and H^2, respectively. In the aliphatic zone, we can observe a singlet at 4.60 ppm ($PhCH_2OH$), two triplets at 4.08 ($PhOCH_2$) and 3.90 ppm ($PhOCH_2$) due to the tetra(ethylene glycol) chain and aliphatic chain, respectively. In addition, we can perceive a singlet at 3.87 ppm ($PhOCH_3$) and a triplet at 3.82 ppm (CH_2N), followed by a multiplet at 3.69–3.62 ppm related to the protons OCH_2 of the oligo(ethylene glycol) segments as well as a singlet at 3.11 ppm (NCH_3). Finally, the protons corresponding to methylenes (CH_2) present in the aliphatic chain appear at 1.74, 1.42, 1.34–1.36 and 0.88 ppm.

The ^{1}H NMR spectrum of dendrimer **14G$_1$** is very similar, we can observe two signals at 8.87 and 5.29 ppm in the aromatic region, due to the protons H^8 and H^o respectively (Fig. 2a). The signals corresponding to the protons present in the azobenzene unit and the phenyl group appear at the same shift as those of **10G$_1$OH**. Finally in the aliphatic region we can observe the same signals perceived for the aliphatic protons between 1.75 and 0.88 ppm (SI, Fig. S6).

The ^{13}C spectrum of **14G$_1$** is illustrated in the Fig. 2b. As we can see, there are 17 signals in aromatic region at 164.72, 160.82, 160.50, 160.11, 150.99, 147.38, 143.60, 137.55, 134.91, 131.21, 124.65, 123.82, 114.09, 111.49, 107.08, 106.62, 101.36 ppm due to the 17 types of aromatic carbons present in the structure of the dendrimer. Moreover, in the aliphatic region we can observe various peaks at 70.75–70.62, 69.60, 67.41 ppm, due to the methylenes present in the tera(ethylene glycol) spacers. The carbons $PhOCH_2$ of the oligo(ethylene glycol) and the aliphatic chain appear at 68.49 and 68.09 ppm, respectively. Four more signals can be perceived at 67.24, 55.45, 52.15 and 39.20 ppm, corresponding to carbons C^o, NCH_2, OCH_3 and NCH_3, respectively. Finally, the signals due to all the CH_2 and CH_3 present in the alphatic chain appear at 31.88, 29.64–29.20, 26.01, 22.65, 14.10 ppm (SI, Fig. S7). The structure and purity of these dendrimers were confirmed by MALDI-TOF mass spectrometry. All dendrimers showed a molecular ion peak which is in agreement with their calculated molecular weight.

4. Optical properties of the dendrimers

Optical properties of the azodendrimers in $CHCl_3$ and DMF solution were studied by absorption spectroscopy in the UV–vis region and the results are summarized in Table 1. The optical data of the dendrons employed as intermediates in the synthesis have been previously reported. The absorption spectra were normalized for a better comparison. In general, the absorption bands of the dendrimers did not show any significant shift with respect to those of the precursor dendrons. However, we can observe a solvatochromic effect; for instance azodendrimer **13G$_1$**, which is high

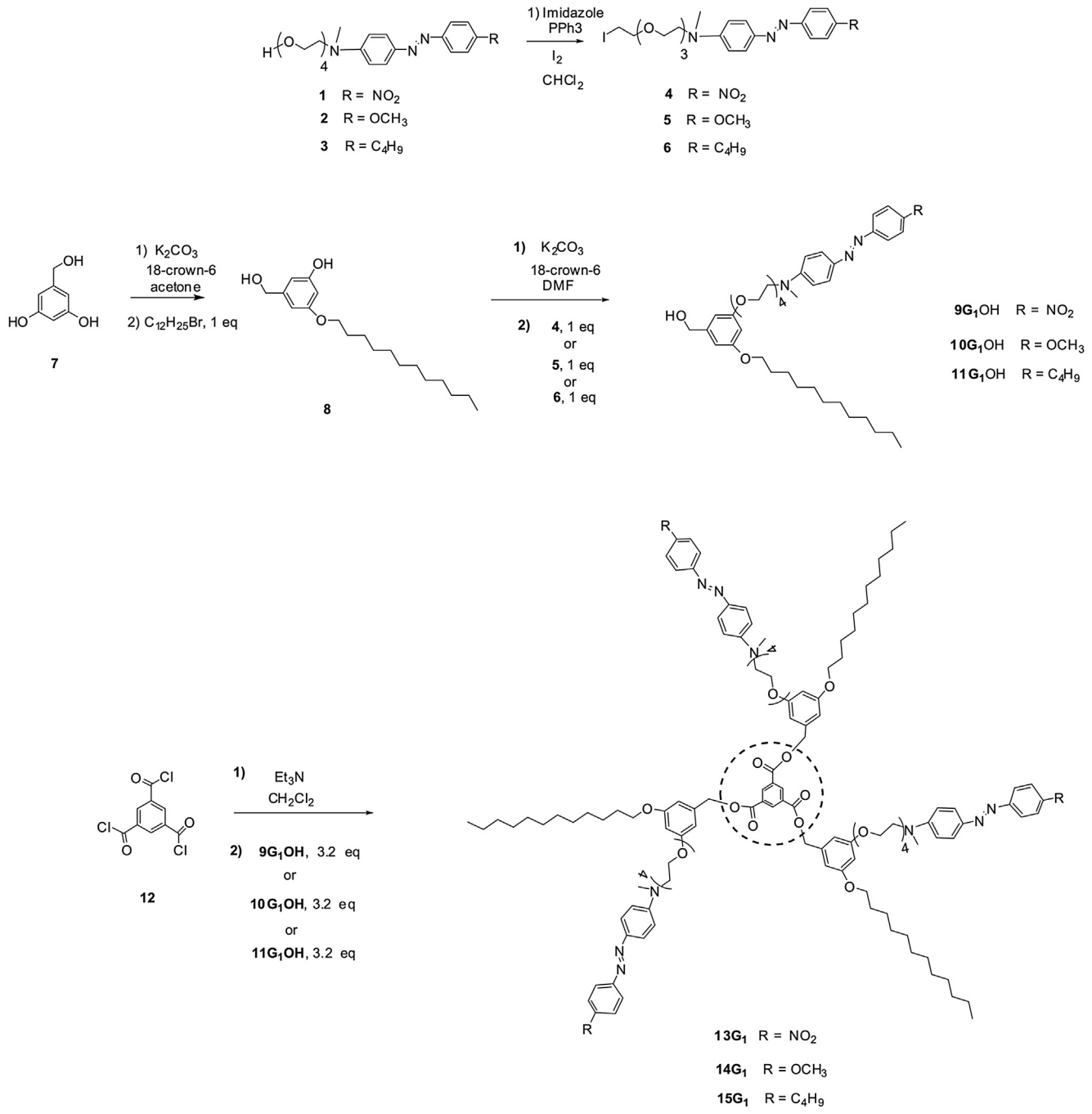

Fig. 1. Synthesis of the first-generations dendrimers.

dipole moment dendrimer bearing amino-nitro substituted azobenzenes, showed a maximum absorption band at $\lambda_{max} = 480$ nm in $CHCl_3$ solution, whereas in DMF solution the absorption band was red-shifted to $\lambda_{max} = 498$ nm (Fig. 3). This compound belong to the pseudostilbenes category, so that it exhibits a total overlap of the $\pi-\pi^*$ and $n-\pi^*$ bands, so that only one band can be observed in the UV–vis spectra. In contrast, low dipole moment dendrimers **14G$_1$** (amino-methoxy) and **15G$_1$** (amino-butyl), exhibited blue-shifted absorption bands with respect to **13G$_1$**. They exhibited maximum absorption band at $\lambda_{max} = 409$ nm followed by a shoulder at $\lambda_{max} = 423$ nm due to the $\pi-\pi^*$ and $n-\pi^*$ transitions, respectively. In DMF solution, a significant red-shift was observed for **14G$_1$** and **15G$_1$** so that the maximum absorption band appeared at 418 nm and the shoulder at 453 nm (Fig. 3). Since these compounds belong to the aminoazobenzenes category they show a partial overlap of the $\pi-\pi^*$ and $n-\pi^*$ bands in their UV–vis spectra.

5. Protonation effect upon irradiation

When all the dendrimers were irradiated for 5 min with UV light at 365 nm in chloroform solution, they did not show any changes in their spectra absorption. However, when they were exposed to the UV lamp at 254 nm the absorption band at 409 nm decreased drastically in intensity, whereas a very intense band appeared at 560 nm. This photochromic effect was monitored by recording

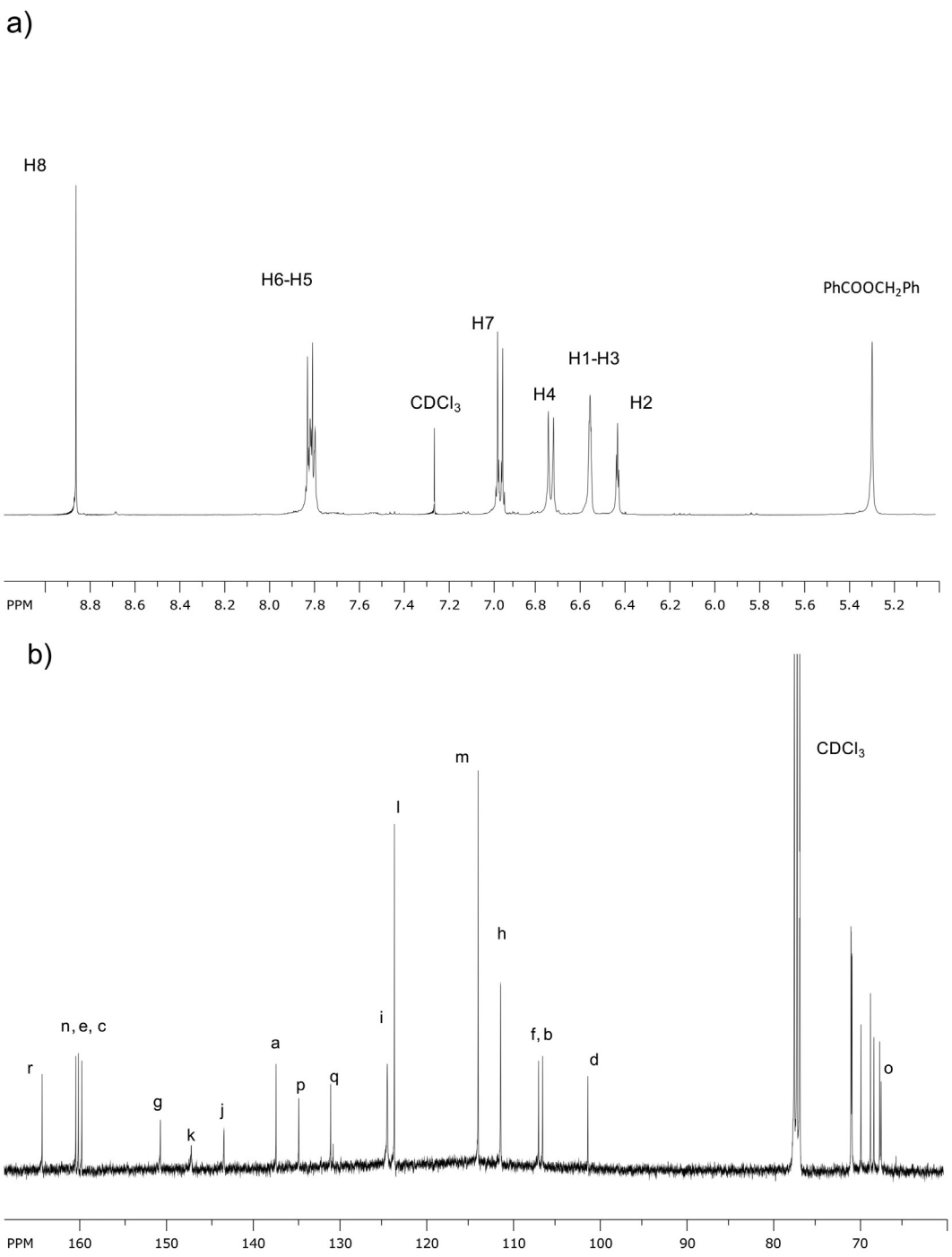

Fig. 2. a) ^{1}H NMR spectral. b) ^{13}C NMR spectral of the dendrimer **$14G_1$** in $CDCl_3$ disolvent.

Table 1
Optical properties of the dendrimers.

Dendrimers	In $CHCl_3$ solution		In DMF solution	
	λ_{max} (nm)	Cut off (nm)	λ_{max} (nm)	Cut off (nm)
$13G_1$	480	600	493	621
$14G_1$	409	525	418	549
$15G_1$	409	525	418	549

absorption spectra every 5 s. Since the extinction coefficient of the n–π^* band is very low the appearance of this new band cannot be attributed to *trans–cis* photoisomerization itself. Moreover, this band can be also observed in azodendrimer **$13G_1$** (amino-nitro) which behaves as a pseudostilbene, where both the π–π^* and n–π^* bands are totally overlapped so that it is not possible to monitor a *trans–cis* photoisomerization for this kind of azo-compounds.

The absorption spectrum of azodendrimer **$13G_1$** (amino-nitro) (not shown) exhibited these chromic changes reaching a photostationary state (PSS) after 200 s of irradiation. After this time two absorption bands were observed: the first one at 523 nm and the

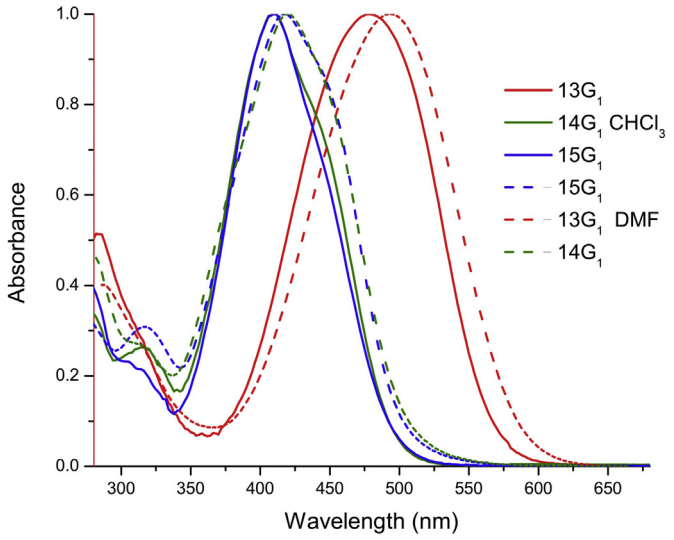

Fig. 3. Normalized absorption spectral of the azodendrimers in $CHCl_3$ and DMF solution.

second one (new) at 550 nm. In contrast, for azodendrimer **$14G_1$** (amino-methoxy) (Fig. 4) the new absorption band due to photoprotonation appears at 560 nm, reaching a photostationary state (PSS) after 45 s. Finally, azodendrimer **$15G_1$** (amino-butyl) behaved similarly, the absorption band at 409 nm decreased in intensity whereas a new absorption band due to photoprotonation increased gradually in intensity at 560 nm; in this case the PSS was attained after 55 s. Additionally these compounds exhibited drastic colour changes along the photoprotonation process. For low dipole moment dendrimers **$14G_1$** and **$15G_1$** a colour change from yellow to pink was observed, whereas for the highly polar dendrimer **$13G_1$** a colour change from red to pink was seen. This colour change can be attributed to the azo-hydrazone tautomerism showed by the amino-azobenzenes derivatives. A similar behaviour was observed in the absorption spectra of some fullerene containing azobenzene derivatives after protonation, which confirmed our hypothesis [66]. In fact, the *trans–cis* photoisomerization and the photoprotonation can occur simultaneously but the effect of the second is more visible in the absorption spectra. Therefore, our dendrimers exhibited an efficient photoprotonation in the presence of a slightly acidic solvents such as $CHCl_3$ (pKa = 15.5). In contrast, when the same irradiation experiments were carried out in the presence of a non acidic solvent such as DMF *trans–cis* occurred in the absence of protonation as expected.

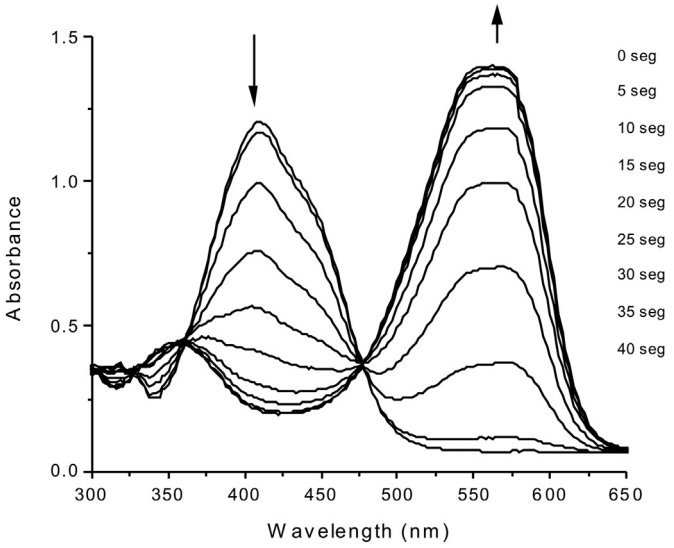

Fig. 4. Photoprotonation effect in **$14G_1$** upon irradiation in function of time.

6. Trans–cis photoisomerization

Photoisomerization experiments were performed with all dendrimers in DMF solution by irradiating with UV light at 365 and 254 nm for 5 min. Low dipole moment azodendrimers **$14G_1$** and **$15G_1$** exhibited a *trans* (E) to *cis* (Z) isomerization. This phenomenon was monitored by absorption spectroscopy every 5 s. In the case of azodendrimer **$13G_1$** the sample was not monitored since kind of azobenzenes show a total overlap of the $\pi-\pi^*$ and $n-\pi^*$ bands. In contrast, low dipole moment azodendrons showed also *trans–cis* photoisomerization when they were irradiated with UV light. The maximum absorption band of **$14G_1$** gradually decreases in intensity upon irradiation since the extinction coefficient of the *cis* isomer is significantly lower (Fig. 5a). This is an indication of the configuration change from the *trans* (E) to the *cis* (Z) isomer. A photostationary state (PSS) was after 45 s of irradiation when all the azobenzenes completely switched to the Z form.

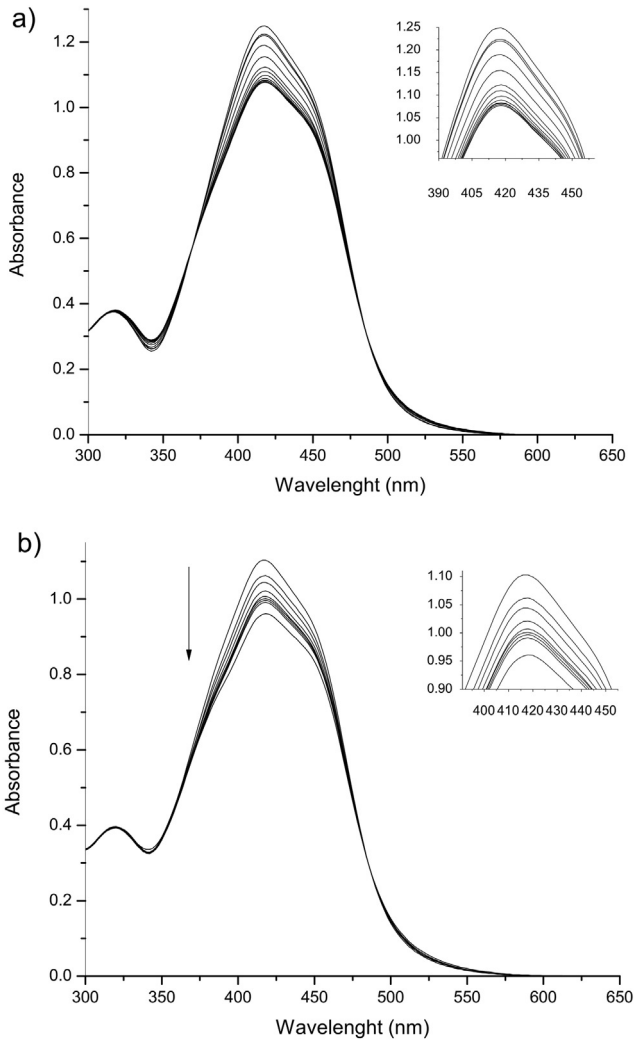

Fig. 5. UV–vis changes spectral in *trans* to *cis* conversion of azodendrimer **$14G_1$**. a) Upon irradiation at 365 nm. b) At 254 nm, for 60 s.

The same behaviour was observed upon irradiation at 254 nm, the maximum absorption band decreases continuously in intensity and the PPS was achieved in 55 s (Fig. 5b). In the plot Ln (abs) versus time for the azodendrimer bearing amino-methoxy substituted azobenzenes has similar characteristics when was irradiated at these two wavelengths (Fig. 6). The decay of the conversion from E to Z isomer in the first 20 s exhibited an exponential increase. In the first time interval the conversion from E to the Z form was faster, furthermore the conversion resulted to be slower. However, the opposite behaviour was observed upon irradiation at 254 nm. In the first 5 s the conversion from the E to the Z isomer occurred much faster.

Finally, the azodendrimer **15G$_1$** behaved as **14G$_1$** (Fig. 7). The *trans*–*cis* photoisomerization of the dendrimer bearing amino-butyl substituted azobenzene was totally achieved in 60 s by irradiating at 365 nm, whereas at 254 nm the conversion occurred in only 5 s. Since **14G$_1$** and **15G$_1$** belong to the aminoazobenzenes category a partial overlap of the $\pi-\pi^*$ and $n-\pi^*$ bands can be observed, where the first one is more intense in intensity. Upon irradiation a significant decrease in intensity of the $\pi-\pi^*$ band was observed thereby indicating that *trans*–*cis* isomerization occurred. Changes in the $n-\pi^*$ band were not noticeable since this band appears as a shoulder.

7. Molecular modelling of the dendrimers

Compound **13G$_1$** was selected as an example for a theoretical study. Fig. 8 shows the most stable optimized structures for *trans* and *cis* isomers of **13G$_1$**. The planar reported structures were used as initial geometries to analyse the *trans*–*cis* isomerization. Initial geometries present well defined *cis* or *trans* azobenzene groups.

Optimized structures of *cis* and *trans* isomers of the dendrimers are quite similar. In fact, the main difference is on the side chain that is twisted in the *trans* isomers in order to reduce the steric hindrance. Both are not planar molecules, with the chains separated and forming a windmill-like structure. The centre of the molecule is planar in both isomers, and in both structures the chains are separated to avoid any steric hindrances.

The *cis*–*trans* energy difference of **13G$_1$** is about 40 kcal/mol, being the *trans* isomer the most stable. There is a remarkable difference between the dipole moments of both isomers. For **13G$_1$**, *trans* isomer, it is 4.10 D whereas for the *cis* isomer it is 15.64 D. This difference is due to the orientation of the substituents in the azobenzene unit. In the *trans* isomer of **13G$_1$** the amino-nitro substituted azobenzenes are oriented up and down while in the *cis* isomer all azobenzenes are oriented in the same direction.

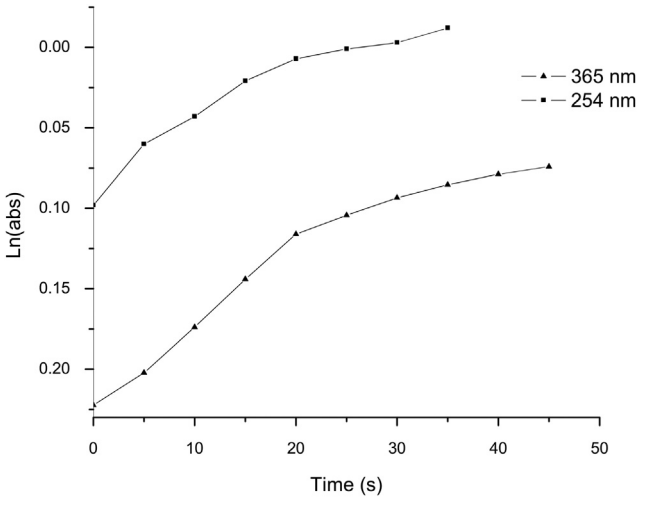

Fig. 6. Ln(abs) versus time plot for change absorbance of the azodendrimer **14G$_1$**.

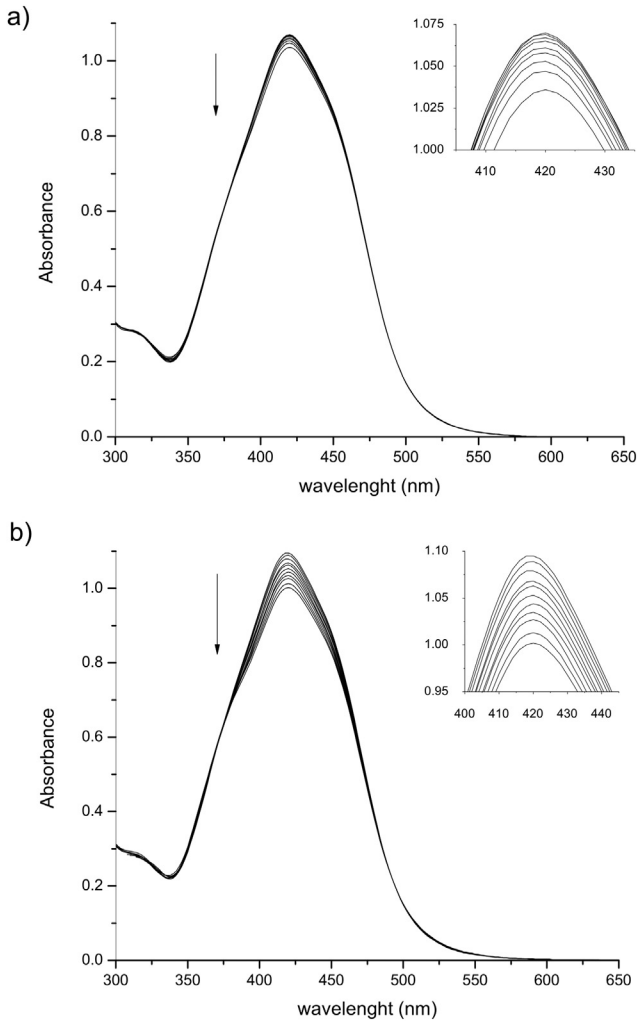

Fig. 7. Absorption spectral changes after irradiation with UV lamp of the azodendrimer **15G$_1$**. a) Upon irradiation at 365 nm. b) Upon irradiation at 254 nm, for 60 s.

The theoretical UV–vis spectra of the *trans* and *cis* isomers of **13G$_1$** are illustrated in Fig. 9. As we can see, there is a significant overlap between both spectra but there is also a significant shift in the maximum absorption bands. For the *trans* isomer, the maximum absorption appears at $\lambda = 475$ nm, and for the *cis* isomer at $\lambda = 540$ nm. In the experimental UV–vis spectrum of **13G$_1$** we can observe a broad absorption band centred at 480–500 nm, since the $\pi-\pi^*$ and the $n-\pi^*$ are very close to each other and practically superimposed. Thus, the theoretical results are in good agreement with those obtained experimentally.

8. Conclusions

Three novel Frechet type dendrimers bearing a well defined oligo(ethylene glycol) side chain and amino-nitro (**13G$_1$**), amino-methoxy (**14G$_1$**) and amino-butyl (**15G$_1$**) substituted azobenzenes were successfully synthesized and characterized. The optical properties of the azodendrimers were studied in $CHCl_3$ and DMF solution by absorption spectroscopy in the UV–vis region. **13G$_1$** which has amino-nitro substituted azobenzenes, showed a maximum absorption band at $\lambda_{max} = 480$ nm in $CHCl_3$ solution,

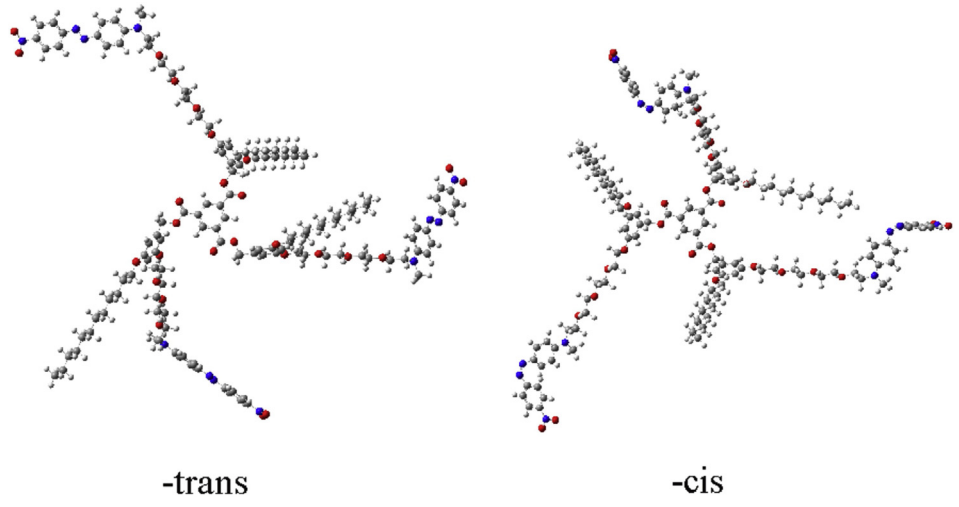

Fig. 8. Optimized structures for the all azodendrimers **13G$_1$**, **14G$_1$** and **15G$_1$**.

which was red-shifted to λ_{max} = 498 nm in DMF solution. This compound exhibits a total overlap of the π–π* and n–π* bands. In contrast, **14G$_1$** (amino-butyl) and **15G$_1$** (amino-methoxy) exhibited maximum absorption band at λ_{max} = 409 nm followed by a shoulder at λ_{max} = 423 nm due to the π–π* and n–π* transitions. These compounds belong to the aminoazobenzenes category they show a partial overlap of the π–π* and n–π* bands in their UV–vis spectra. The obtained results fitted well with those predicted by molecular modelling.

Photoisomerization experiments were performed with all dendrimers in DMF solution by irradiating with UV light at 365 and 254 nm. Low dipole moment azodendrimers **14G$_1$** and **15G$_1$** exhibited a *trans* (E) to *cis* (Z) isomerization. This phenomenon was monitored by absorption spectroscopy. A photostationary state (PSS) was after 45 s of irradiation when all the azobenzenes completely switched to the *Z* form. The same behaviour was observed upon irradiation at 254 nm, the maximum absorption band decreases continuously in intensity and the PPS was achieved in 55 s.

When the irradiation experiments were conducted in $CHCl_3$, all dendrimers exhibited photochromic changes due to the photoprotonation of the azobenzene unit. This was confirmed by a significant the red-shift of the maximum absorption band (ca. λ = 523 nm) followed by the appearance of a very intense red shifted band (ca. λ = 560 nm). A colour change from red to pink due to the azo-hydrazone tautomerism was also observed.

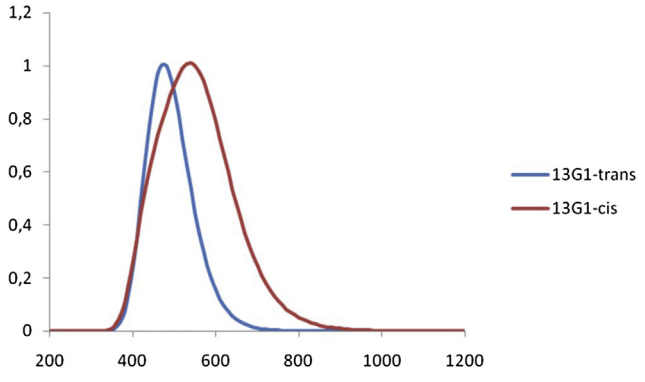

Fig. 9. Absorption spectra theoretically predicted for the *trans* and *cis* isomers of dendrimer **13G$_1$**.

Acknowledgements

We are grateful to Miguel Angel Canseco for his assistance with UV–vis spectroscopy and Gerardo Cedillo for his help with ^{1}H and ^{13}C NMR spectroscopy. This project was financially supported by PAPIIT (Project IN-100513). This study was also funded by Consejo Nacional de Ciencia y Tecnología (CONACyT Project 128788) and resources provided by the Instituto de Investigaciones en Materiales (IIM). Theoretical calculations were carried out using a NES (Miztli) supercomputer, provided by Dirección General de Cómputo y Tecnologías de Información y Comunicación (DGTIC).

Appendix A. Supplementary data

Supplementary data related to this article can be found at http://dx.doi.org/10.1016/j.dyepig.2014.11.023.

References

[1] Fréchet JMJ, Tomalia D. Dendrimers and other dendritic polymers. New York: Wiley; 2002.
[2] Newkome GR, Vögtle F, Moorefield CN. Dendrimers and dendrons. Weinheim, Germany: Wiley-VCH; 2001.
[3] Newkome GR, Shreiner CD. Poly(amidoamine), polypropylenimine, and related dendrimers and dendrons possessing different 1/2 branching motifs: an overview of the divergent procedures. Polymer 2008;49:1–173. http://www.sciencedirect.com/science/article/pii/S0032386107010154.
[4] Jean-Pierre Majoral, Anne-Marie Caminade. Dendrimers containing heteroatoms (Si, P, B, Ge, or Bi). ChemRev 1999;99:845–80. http://pubs.acs.org/doi/abs/10.1021/cr970414j?journalCode=chreay&quickLinkVolume=99&quickLinkPage=845&selectedTab=citation&volume=99.
[5] Vögtle F, Richardt G, Werner N. Dendrimer chemistry. Weinheim, Germany: Wiley-VCH; 2009.
[6] Momotake A, Arai T. Synthesis, excited state properties, and dynamic structural change of photoresponsive dendrimers. Polymer 2004;45:5369–90. http://www.sciencedirect.com/science/article/pii/S0032386104005713.
[7] Momotake A, Arai T. Photochemistry and photophysics of stilbene dendrimers and related compounds. J Photochem Photobiol C Photochem Rev 2004;5:1–25. http://www.sciencedirect.com/science/article/pii/S1389556704000024.
[8] Shibaev V, Bobrovsky A, Boiko N. Photoactive liquid crystalline polymer systems with light-controllable structure and optical properties. Prog Polym Sci 2003;28:729–836. http://www.sciencedirect.com/science/article/pii/S0079670002000862.
[9] Villavicencio O, McGrath DV. In: Newkome George R, editor. Advances in dendritic macromolecules, vol. 5; 2002. p. 1–44.
[10] Deloncle R, Anne-Marie Caminade. Stimuli-responsive dendritic structures: the case of light-driven azobenzene-containing dendrimers and dendrons. J Photochem Photobiol C Photochem Rev 2010;11:25–45. http://www.sciencedirect.com/science/article/pii/S1389556710000201.
[11] Mekelburger HB, Rissanen K, Vögtle F. Repetitive-synthesis of bulky dendrimers – a reversibly photoactive dendrimers with six azobenzene side

chains. Chem Ber 1993;126:1161–9. http://onlinelibrary.wiley.com/doi/10.1002/cber.19931260516/abstract.
[12] Buhleier EW, Wehner W, Vögtle F. Cascade and nonskid-chain-like syntheses of molecular cavity topologies. Synthesis 1978;2:155–8. https://www.thieme-connect.com/ejournals/abstract/10.1055/s-1978-24702.
[13] Wörner C, Mülhaupt R. Polynitrile and polyamine funtional poly(trimethylene imine) dendrimers. Angew Chem Int Ed Engl 1993;32:1306–8. http://onlinelibrary.wiley.com/doi/10.1002/anie.199313061/abstract.
[14] De Brabander-van den Berg EMM, Meijer EW. Poly(propylene imine) dendrimers: large-scale synthesis by hetereogeneously catalyzed hydrogenations. Angew Chem Int Ed Engl 1993;32:1308–11. http://onlinelibrary.wiley.com/doi/10.1002/anie.199313081/abstract.
[15] Archut A, Vögtle F, De Cola L, Azzellini GC, Balzani V, Ramanujam PS, et al. Azobenzene-functionalized cascade molecules: photoswitchable supramolecular systems. Chem Eur J 1998;4:699–706. http://onlinelibrary.wiley.com/doi/10.1002/%28SICI%291521-3765%2819980416%294:4%3C699::AID-CHEM699%3E3.0.CO;2-9/abstract.
[16] Dirksen A, Zuidema E, Williams RM, De Cola L, Kauffmann C, Vögtle F, et al. Photoactivity and pH sensitivity of methyl orange functionalized poly(propyleneamine) dendrimers. Macromolecules 2002;35:2743–7. http://pubs.acs.org/doi/abs/10.1021/ma011350o?journalCode=mamobx&quickLinkVolume=35&quickLinkPage=2743&selectedTab=citation&volume=35.
[17] Schenning AP, Elissen-Roman C, Weener JW, Baars MW, Van der Gaast SJ, Meijer EW. Amphiphilic dendrimers as building blocks in supramolecular assemblies. J Am Chem Soc 1998;120:8199–208. http://pubs.acs.org/doi/abs/10.1021/ja9736774?journalCode=jacsat&quickLinkVolume=120&quickLinkPage=8199&selectedTab=citation&volume=120.
[18] Alcala R, Gimenez R, Oriol L, Pinol M, Serrano JL, Villacampa B, et al. Synthesis, characterization, and induction of stable anisotropy in liquid crystalline photo-addressable PPI dendrimers. Chem Mater 2007;19:235–46. http://pubs.acs.org/doi/abs/10.1021/cm061727a?journalCode=cmatex&quickLinkVolume=19&quickLinkPage=235&selectedTab=citation&volume=19.
[19] Tomalia DA, Baker H, Dewald J, Hall M, Kallos G, Martin S, et al. A new class of polymers: starburts-dendritic macromolecules. Polym J 1985;17:117–32. http://www.nature.com/pj/journal/v17/n1/abs/pj198510a.html.
[20] Hawker CJ, Fréchet JMJ. Preparation of polymers with controlled molecular architecture. A new convergent approach to dendritic macromolecules. J Am Chem Soc 1990;112:7638–47. http://pubs.acs.org/doi/abs/10.1021/ja00177a027?journalCode=jacsat&quickLinkVolume=112&quickLinkPage=7638&selectedTab=citation&volume=112.
[21] Li S, McGrath DV. Macromolecular isomers of azobenzene-containing photochromic dendrimers. Polym Prep Am Chem Soc Div Polym Chem 2000;41:861–4. http://www.polyacs.org/.
[22] Li S, McGrath DV. Effect of macromolecular isomerism on the photomodulation of dendrimer properties. J Am Chem Soc 2000;122:6795–6. http://pubs.acs.org/doi/abs/10.1021/ja0015085?journalCode=jacsat&quickLinkVolume=122&quickLinkPage=6795&selectedTab=citation&volume=122.
[23] Nithyanandhan J, Jayaraman N, Davis R, Das S. Synthesis, fluorescence and photoisomerization studies of azobenzene-functionalized poly(alkyl aryl ether) dendrimers. Chem Eur J 2004;10:689–98. http://onlinelibrary.wiley.com/doi/10.1002/chem.200305297/abstract.
[24] Kay KY, Han KJ, Yu YJ, Park YD. Dendritic fullerenes (C_{60}) with photoresponsive azobenzene groups. Tetrahedron Lett 2002;43:5053–6. http://www.sciencedirect.com/science/article/pii/S0040403902009942.
[25] Rau H. In: Rabek JK, editor. Photochemistry and photophysics, vol. 2. Boca Raton, Florida: CRC Press; 1990. p. 119.
[26] Natansohn A, Rochon P. 2000 macromolecular science and engineering award lecture the versatility of azobenzene polymers. Can J Chem 2001;79:1093–100. http://www.nrcresearchpress.com/doi/abs/10.1139/v01-098#.U0Q99nas-UI.
[27] Todorov T, Nikalova L, Tomova N. Polarization holography. 1: a new high-efficiency organic material with reversible photoinduced birefringence. Appl Opt 1984;23:4309–12. http://www.opticsinfobase.org/ao/abstract.cfm?URI=ao-23-23-4309.
[28] Xie S, Natansohn A, Rochon P. Recent developments in aromatic azo polymers research. Chem Mater 1993;5:403–11. http://pubs.acs.org/doi/abs/10.1021/cm00028a003?journalCode=cmatex&quickLinkVoume=5&quickLinkPage=403&selectedTab=citation&volume=5.
[29] Viswanathan NK, Kim DY, Bian S, Williams J, Liu W, Li L, et al. Surface relief structures on azo polymer films. J Mater Chem 1999;9:1941–55. http://pubs.rsc.org/en/content/articlelanding/1999/jm/a902424g#!divAbstract.
[30] Ichimura K. Photoalignment of liquid-crystal systems. Chem Rev 2000;100:1847–74. http://pubs.acs.org/doi/abs/10.1021/cr980079e?journalCode=chreay&quickLinkVolume=100&quickLinkPage=1847&selectedTab=citation&volume=100.
[31] Delaire JA, Nakatani K. Linear and nonlinear optical properties of photochromic molecules and materials. Chem Rev 2000;100:1817–46. http://pubs.acs.org/doi/abs/10.1021/cr980078m?journalCode=chreay&quickLinkVolume=100&quickLinkPage=1817&selectedTab=citation&volume=100.
[32] Natansohn A, Rochon P. Photoinduced motions in azo containing polymers. Chem Rev 2002;102:4139–75. http://pubs.acs.org/doi/abs/10.1021/cr970155y?journalCode=chreay&quickLinkVolume=102&quickLinkPage=4139&selectedTab=citation&volume=102.
[33] Kasha M. Energy transfer mechanisms and the molecular exciton model for molecular aggregates. Radiat Res 1963;20:55–71. http://www.rrjournal.org/doi/abs/10.2307/3571331?journalCode=rare.
[34] He X, Zhang HL, Yan DL, Wang X. Synthesis of side-chain liquid-crystalline homopolymers and triblock copolymers with *p*-methoxyazobenzene moieties and poly(ethylene glycol) as coil segments by atom transfer radical polymerization and their thermotropic phase behavior. J Polym Sci Part A Polym Chem 2003;41:2854–64. http://onlinelibrary.wiley.com/doi/10.1002/pola.10870/abstract.
[35] Tian YQ, Watanabe K, Kong XX, Abe J, Iyoda T. Synthesis, nanostructures, and functionality of amphiphilic liquid crystalline block copolymers with azobenzene moieties. Macromolecules 2002;35:3739–47. http://pubs.acs.org/doi/abs/10.1021/ma011859j?journalCode=mamobx&quickLinkVolume=35&quickLinkPage=3739&selectedTab=citation&volume=35.
[36] Saito M, Shimomura T, Okumura Y, Ito K, Hayakawa R. Temperature dependence of inclusion-dissociation behavior between molecular nanotubes and linear polymers. J Chem Phys 2001;114:1–3. http://scitation.aip.org/content/aip/journal/jcp/114/1/10.1063/1.1334599.
[37] Shimomura T, Funaki T, Ito K. Circular dichroism study of the inclusion-dissociation behavior of complexes between a molecular nanotube and azobenzene substituted linear polymers. J Incl Phenom Macroc Chem 2002;44:275–8. http://link.springer.com/article/10.1023/A%3A1023032632076.
[38] Zheng PJ, Wang C, Hu X, Tam KC, Li L. Supramolecular complexes of azocellulose and R-cyclodextrin: isothermal titration calorimetric and spectroscopic studies. Macromolecules 2005;38:2859–64. http://pubs.acs.org/doi/abs/10.1021/ma048324l?journalCode=mamobx&quickLinkVolume=38&quickLinkPage=2859&selectedTab=citation&volume=38.
[39] Hu X, Zheng PJ, Zhao XY, Li L, Tam KC, Gan LH. Preparation, characterization and novel photoregulated rheological properties of azobenzene functionalized cellulose derivatives and their α-CD complexes. Polymer 2004;45:6219–25. http://www.sciencedirect.com/science/article/pii/S0032386104005695.
[40] Takashima Y, Nakayama T, Miyauchi M, Kawaguchi Y. Complex formation and gelation between copolymers containing pendant azobenzene groups and cyclodextrin polymers. Chem Lett 2004;33:890–1. https://www.jstage.jst.go.jp/article/cl/33/7/33_7_890/_article.
[41] Ikeda T, Ooya T, Yui N. Regulation of pseudo-polyrotaxane formation between α-cyclodetrins and azobenzene-terminated poly(ethylene glycol). Polym J 1999;31:658–63. http://www.nature.com/pj/journal/v31/n8/abs/pj1999123a.html.
[42] Tung CH, Wu LZ, Zhang LP, Chen B. Supramolecular systems as microreactors: control of product selectivity in organic phototransformation. Acc Chem Res 2003;36:39–47. http://pubs.acs.org/doi/abs/10.1021/ar010141l?journalCode=achre4&quickLinkVolume=36&quickLinkPage=39&selectedTab=citation&volume=36.
[43] Rivera E, Belletête M, Natansohn A, Durocher G. Synthesis characterization and optical properties of a novel azo-dye bearing an oligo(ethylene glycol) methyl ether side chain in solution and in the solid state. Can J Chem 2003;81:1076–82. http://www.nrcresearchpress.com/doi/abs/10.1139/v03-136#.U0RC7Xas-UI.
[44] Rivera E, Carreón-Castro MP, Buendía I, Cedillo G. Optical properties and aggregation of novel azo-dyes bearing an end-capped oligo(ethylene glycol) side chain in solution, solid state and Langmuir-Blodgett films. Dyes Pigments 2006;68:217–26. http://www.sciencedirect.com/science/article/pii/S0143720805000872.
[45] Rivera E, Carreón-Castro MP, Salazar R, Huerta G, Becerril C, Rivera L. Preparation and characterization of novel grafted polyethylene based azo-polymers bearing oligo(ethylene glycol) spacers. Polymer 2007;48:3420–8. http://www.sciencedirect.com/science/article/pii/S0032386107004144.
[46] García T, Carreón-Castro MP, Gelover-Santiago A, Ponce P, Romero M, Rivera E. Synthesis and characterization of novel amphiphilic azo-polymers bearing well-defined oligo(ethylene glycol) spacers. Des Monomers Polym 2012;15:159–74. http://www.tandfonline.com/doi/abs/10.1163/156855511X615047#.U0REKXas-UI.
[47] Caicedo C, Rivera E, Valdez-Hernández Y, Carreón-Castro MP. Synthesis and characterization of novel liquid-crystalline azo-dyes bearing two amino-nitro substituted azobenzene units and a well-defined, oligo(ethylene glycol) spacer. Mater Chem Phys 2011;130:471–80. http://www.sciencedirect.com/science/article/pii/S0254058411006055.
[48] Zhu Y, Zhou Y, Wang X. Photoresponsive behavior of two well-defined azo polymers with different electron-withdrawing groups on push-pull azo chromophores. Dyes Pigments 2013;99:209–19. http://www.sciencedirect.com/science/article/pii/S014372081300171X.
[49] Miura Y, Momotake A, Kanna Y, Nishimura Y, Arai T. Extremely efficient photoisomerization of water-soluble diphenylbutadiene dendrimers. Dyes Pigments 2012;92:802–6. http://www.sciencedirect.com/science/article/pii/S0143720811001203.
[50] Bae1 SH, Kim HM, Min HS, Kim D, Kim TD. Crosslinkable nonlinear optical dendrimers synthesized by Diels-Alder reaction. J Nanosci Nanotechnol 2012;12:730–6. http://www.ingentaconnect.com/content/asp/jnn/2012/00000012/00000001/art00106?token=003b16513fec2d5c5f3b3b47466648773b6f7051796c7a414f58762f67e.
[51] Lee JH, Choi D, Shin EJ. *Trans-cis* isomerization of arylether dendrimers with azobenzene core and terminal hydroxy groups. Spectrochim Acta A 2010;77:478–84. http://www.sciencedirect.com/science/article/pii/S1386142510003136.
[52] Galán H, Hennrich G, De Mendoza J, Prados P. Synthesis and photoisomerization of azocalixarenes with dendritic structures. Eur J Org Chem 2010;2010:1249–57. http://onlinelibrary.wiley.com/doi/10.1002/ejoc.200901394/abstract.

[53] Alam MDZ, Ogata T, Kuwahara Y, Kurihara S. Synthesis and characterization of azobenzene-functionalized hyperbranched polymers. Mol Cryst Liq Cryst 2010;529:25–31. http://www.tandfonline.com/doi/full/10.1080/15421406.2010.495658#.U_9-m6NseZQ.

[54] Koyama T, Hatano K, Matsuoka K, Esumi Y, Terunuma D. Synthesis and characterization of photo-responsive carbosilane dendrimers. Molecules 2009;14:2226–34. http://www.mdpi.com/1420-3049/14/6/2226.

[55] Kim DY, Lee SA, Choi YJ, Hwang SH, Kuo SW, Nah C, et al. Thermal and photo-induced phase transition behaviors of a tapered dendritic liquid crystal with photochromic azobenzene mesogens and a bicyclic chiral center. Chem Eur J 2014;20:5689–95. http://onlinelibrary.wiley.com/doi/10.1002/chem.201303924/abstract.

[56] Viñuales AI, Serrano JL, Giménez R, Piñol M, Tomczyk J, Stumpe J. Liquid crystalline dendrimers containing photoactive cinnamate units. J Polym Sci A 2011;49:3499–512. http://onlinelibrary.wiley.com/doi/10.1002/pola.24785/abstract.

[57] Ortíz-Palacios J, Rodríguez-Alba E, Avelar M, Martínez A, Carreón-Castro MP, Rivera Ernesto. Synthesis and characterization of novel dendrons bearing amino-nitro-substituted azobenzene units and oligo(ethylene glycol) spacers: thermal, optical properties, Langmuir blodgett films and liquid-crystalline behaviour. Molecules 2013;18:1502–27. http://www.mdpi.com/1420-3049/18/2/1502.

[58] Alvarez-Venicio V, Jiménez-Nava B, Carreón-Castro MP, Rivera E, Méndez IA, Huerta AA, et al. Synthesis and incorporation in Langmuir films of oligophenylene vinylene dendrimers bearing a polar head group and different dendritic poly(benzyl ether) branches. Polymer 2008;49:3911–22. http://www.sciencedirect.com/science/article/pii/S0032386108005399.

[59] Frisch MJ, Trucks GW, Schlegel HB, Scuseria GE, Robb MA, Cheeseman JR, et al. Gaussian 09, Revision A.08. Wallingford CT: Gaussian, Inc; 2009.

[60] Becke AD. Density-functional thermochemistry. III. The role of exact exchange. J Chem Phys 1993;98:5648–52. http://scitation.aip.org/content/aip/journal/jcp/98/7/10.1063/1.464913.

[61] Ditchfield R, Hehre WJ, Pople JA. Self-consistent molecular orbital methods. 9. Extended Gaussian-type basis for molecular-orbital studies of organic molecules. J Chem Phys 1971;54:724–8. http://scitation.aip.org/content/aip/journal/jcp/54/2/10.1063/1.1674902.

[62] Hehre WJ, Ditchfield R, Pople JA. Self-consistent molecular orbital methods. 12. Further extensions of Gaussian-type basis sets for use in molecular-orbital studies of organic-molecules. J Chem Phys 1972;56:2257–61. http://scitation.aip.org/content/aip/journal/jcp/56/5/10.1063/1.1677527.

[63] Hariharan PC, Pople JA. Influence of polarization functions on molecular-orbital hydrogenation energies. Theor Chem Acc 1973;28:213–22. http://link.springer.com/article/10.1007/BF00533485.

[64] Hariharan PC, Pople JA. Accuracy of AH equilibrium geometries by single determinant molecular-orbital theory. Mol Phys 1974;27:209–14. http://www.tandfonline.com/doi/abs/10.1080/00268977400100171#.U0RFwHas-UI.

[65] Francl MM, Pietro WJ, Hehre WJ, Binkley JS, DeFrees DJ, Pople JA, et al. Self-consistent molecular orbital methods. 23. A polarization-type basis set for 2nd-row elements. J Chem Phys 1982;77:3654–65. http://scitation.aip.org/content/aip/journal/jcp/77/7/10.1063/1.444267.

[66] Kumar KS, Patnaik A. Tunable electronic properties of a proton-responsive N,N-dimethylaminoazobenzene fullerene (C_{60}) dyad. Chem Phys Chem 2010;11:3645–55. http://onlinelibrary.wiley.com/doi/10.1002/cphc.201000564/abstract.